

20,000 K component. One can speculate that the spectral variations of April–June 1982 are due to an increase of the flux emitted by the hotter component (increase in area) probably accompanied by a smoothing of the temperature distribution. The hot component may result from the sudden heating of the inner part of an accretion disk. Another speculative possibility is the explosion of a supernova in a large cluster of stars coinciding with the central source. In the wind and shock model<sup>11</sup>, this would cause a heating of one part of the ultraviolet photosphere.

The flare seen in the ultraviolet should manifest itself in other regions of the spectrum. Note that a flare in the millimetre–infrared was observed in 1983, although with a significantly lower energy,  $10^{45}$  erg (ref. 12). It is uncertain whether the two flares are related. This points to the importance of continuous broad-band monitoring of this type of sources, as the observation of a time delay between the flaring at different wavelengths would give precise information on the relations between the different physical components.

The presence of flares in different parts of the spectrum makes the spectral decompositions attempted<sup>1–4</sup> very dependent on the epochs of the measurements at different wavelengths. This effect has yet to be taken into account.

We thank Dr E. Tanzi for supplying the 1984 data and the staff of the ESA Villafranca Tracking Station for reprocessing some spectra. T.J.-L.C. is affiliated to the Astrophysics Division, Space Science Department, European Space Agency.

Received 17 January; accepted 10 June 1985.

1. Shields, G. A. *Nature* **272**, 706–708 (1978).
2. Ulrich, M. H. *Space Sci. Rev.* **28**, 89–104 (1981).
3. Malkan, M. A. *Astrophys. J.* **268**, 582–590 (1983).
4. Camenzind, M. & Courvoisier, T. J.-L. *Astr. Astrophys.* **140**, 341–344 (1984).
5. Boggess, A. *et al.* *Nature* **275**, 372–376 (1978).
6. Wills, B. J., Netzer, H. & Wills, D. *Astrophys. J.* **288**, 94–116 (1985).
7. Wu, C.-C. *Astrophys. J. Lett.* **217**, L117–L120 (1977).
8. Sonneborn, G. & Garhart, M. P. *NASA IUE Newslett.* **23**, 23–30 (1983).
9. Oliverson, N. A. *NASA IUE Newslett.* **23**, 31–43 (1983).
10. Perola, G. C. *et al.* *Mon. Not. R. astr. Soc.* **200**, 293–312 (1982).
11. Camenzind, M. & Courvoisier, T. J.-L. *Astrophys. J. Lett.* **66**, L83–87 (1983).
12. Robson, E. I. *et al.* *Nature* **305**, 194–196 (1983).
13. Kwan, J. *Astrophys. J.* **283**, 70–80 (1984).

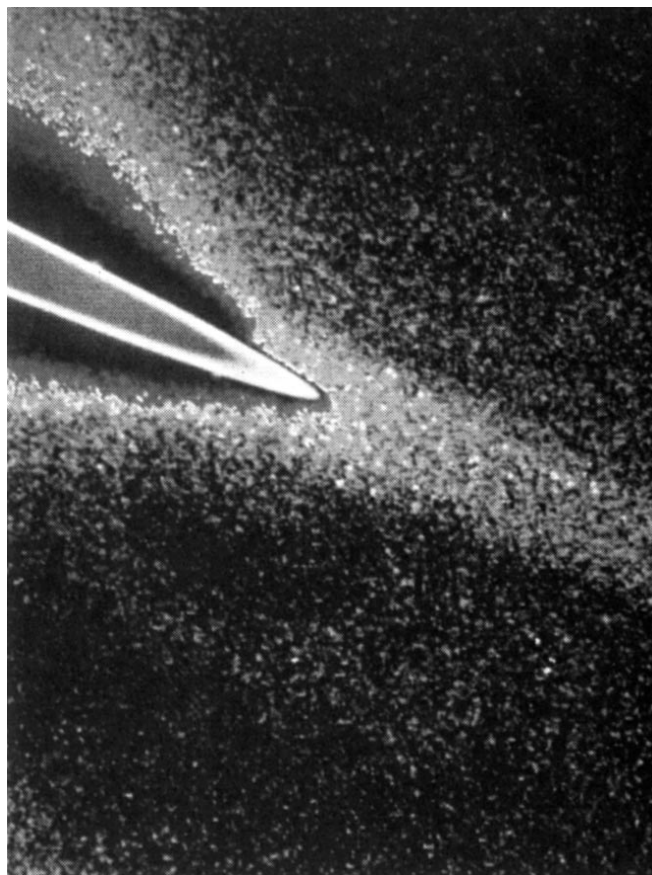


**Fig. 1** An enhancement of Voyager image FDS 20693.02, shown black-and-white above and colour on the cover. Here discrete colours of the spectrum have replaced a range of the darkest shades of grey in the image. The newly-discovered 'gossamer' ring is visible as a blue-green stripe running outward from the bright ring (in white). The halo (outlined in red-yellow) rises at the bright ring's inner edge, and extends vertically above and below the ring.

## Discovery of Jupiter's 'gossamer' ring

Mark R. Showalter\*, Joseph A. Burns\*,  
Jeffrey N. Cuzzi† & James B. Pollack†

\* Center for Radiophysics and Space Research,  
Cornell University, Ithaca, New York 14853, USA  
† NASA/Ames Research Center, Moffett Field, California 94035,  
USA

Jupiter's ring system has previously been described as being composed of a 'bright' narrow ring and an interior, vertically-extended halo<sup>1,2</sup>. The one image which reveals this morphology most clearly is Voyager 2's parting shot of the Jupiter system, a wide-angle (WA) view of the ring ansa in forward-scattered light (FDS 20693.02). The bright ring is plainly visible, and the halo appears after slight contrast enhancement. By further enhancement of this image we have discovered an additional ring, which is far fainter than either of the (already faint) components previously identified, extending to a radius of 210,000 km.

The ring is visible as the blue-green stripe extending outward from the bright ring in Fig. 1. Although this feature has a mean intensity of only one-half the overall image noise level, it covers such a large area ( $\sim 3 \times 10^4$  pixels) that its integrated signal-to-noise ratio is  $\sim 110$ . Previous WA frames were checked to verify that this is not a ghost image, such as are occasionally visible in Voyager data. The lack of systematic variations of this form in any other Voyager images, as well as the consistency of this feature's morphology with a flat circular ring in Jupiter's equator,

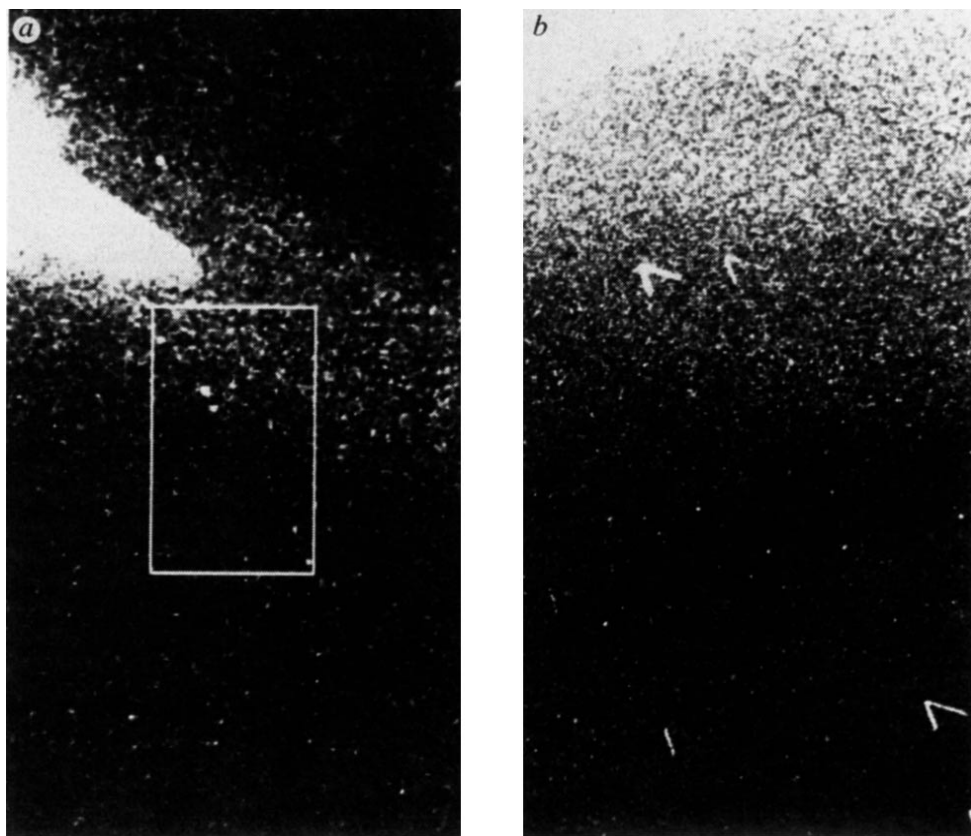
safely rule out the possibility that the stripe is a quirk of the Voyager vidicon.

This particular image has already received extensive scrutiny<sup>2,3</sup> so it may seem surprising that the ring has been overlooked. Raw Voyager images receive extensive reprocessing on the ground, which includes the subtraction of a 'dark current', or image of dark sky, to model the null response of the vidicon. Previous versions of this frame were processed with an inappropriate dark current; this introduced a strong intensity gradient to the dark sky regions of the image, which masked this very subtle feature. We first noted the ring after subtracting an empirical fit to the background of the flawed image data, but found it easily once the image had been reprocessed with an updated dark current.

Only one additional Voyager image captures this ring with tolerable signal-to-noise ratio. The final frame (FDS 20693.01) of a narrow-angle (NA) mosaic accidentally fell beyond the bright ring's ansa, and so captured a piece of this faint structure (Fig. 2). However, the ring contributes only a smooth intensity gradient to the restricted NA field of view, which would have been impossible to interpret unequivocally without the context of the WA frame. Despite some uncertainty in this image's true dark current, it is compatible with the presence of the exterior ring<sup>4</sup>.

In retrospect, the additional ring was hinted at in earlier Pioneer 10 and 11 data. Pioneer 10's meteoroid impact detector recorded at least one event near ring plane crossing at 206,000 km (refs 5, 7), well outside the bright ring but within the ring described here. Since the instrument locks out additional detections for 80 min following an event, the actual number of impacts

**Fig. 2** A comparison of the wide-angle (WA) and narrow-angle (NA) frames. *a*, A portion of the WA frame (FDS 20693.02), contrast-enhanced to show the gossamer ring. The rectangle outlines the corresponding NA field of view. *b*, The NA image (FDS 20693.01), using the same contrast enhancement.



during ring plane crossing is not known. Also, the Pioneer 11 charged particle absorption data, which first detected the bright ring<sup>6</sup>, have never been completely unravelled (W. Fillius, personal communication) but may require additional absorbers between Amalthea and the ring.

Since this 'gossamer' ring is only present at  $0.5\sigma$  in the WA image, extracting its properties may only be accomplished by averaging over large numbers of the available pixels. Figure 3 is a radial profile of the ring, generated by averaging pixel intensities along contours of constant orbital radius. It shows that the ring decreases in intensity rather uniformly with radius; most of it lies inside the orbit of Amalthea, though some material extends out to 210,000 km, and perhaps to the neighbourhood of Thebe. Its overall mean brightness is  $\sim 5\%$  that of the main ring. The profile's only notable feature is a  $\sim 20\%$  enhancement centred at  $160,000 \pm 2,000$  km, quite close to synchronous orbit (160,200 km). This bulge is significant at the  $4\sigma$  level; in fact, it was first observed visually in the image, and only later found to fall on top of a special orbit. This unresolved feature is 5,000-km wide in the scan, but may actually be much narrower and brighter.

The profile of Fig. 3 is produced assuming that the ring is azimuthally symmetric, relatively thin and confined to the equatorial plane. A firm upper limit of 4,000 km may be placed on the ring's vertical extent from the width of the observed stripe at Voyager's shallow viewing angle (a mere  $2^\circ$  from the ring plane); although not severely constrained, this ring is distinctly thinner than the halo. For a ring  $\geq 200$  km thick, lines-of-sight from Voyager would sample a significant range of orbital radii through the ring plane. In this case, vertical structure would be confused with radial structure, and the profile would be in error. However, the synchronous feature must be  $< 200$  km thick to be consistent with its width in the profile.

The ring shows some evidence for a variation in brightness with scattering angle  $\theta$  over the limited range sampled. Intensity at constant orbital radius increases by nearly a factor of two between  $\theta = 7^\circ$  and  $6^\circ$ , suggesting diffraction by grains of radius  $r \approx 1.5 \mu\text{m}$  (Fig. 4). Although this strongly implies the presence of micrometre-sized grains, as in the main ring<sup>2,4</sup>, it is not

possible to exclude the presence of either larger or smaller particles based on such a tiny range of  $\theta$  (ref. 1). If the constituent particle size distribution is the same as that in the bright ring, then this ring's normal optical depth  $\tau \approx 10^{-7}$ , which is comparable to that of Saturn's E ring, another ring known for its small grain population<sup>1</sup>. This value is compatible with  $\tau \approx 10^{-8}$ , determined from the Pioneer 10 impact detection near the ring's outer boundary, and applying only to particles larger than  $r \approx 6 \mu\text{m}$ .

We have failed to detect this ring in the three available backscattered views of the main ring's terminus (FDS 16368.19, 20630.52, 20630.53), despite averaging over many pixels; in these images, the exterior ring must be  $< 1\%$  as bright as the main ring. This limit is smaller than the rings' forward-scatter intensity ratio of  $\sim 5\%$ , which suggests that the gossamer ring contains relatively fewer particles large enough ( $r \gg 1 \mu\text{m}$ ) to backscatter efficiently<sup>4</sup>.

The dominant evolutionary process acting to move jovian ring material is plasma drag<sup>1</sup>. This force arises from collisions with plasma, which is tied to the planet's rotating magnetic field; it evolves material away from synchronous orbit, either inward or outward, on timescales of  $\sim 10^3 \pm 1$  yr for micrometre-sized grains. The dominant destruction process, sputtering, acts on similar timescales for these tiny grains<sup>1</sup>.

Given such brief lifetimes, ring material must be continually replenished from some source for the ring to remain visible today. The alternative, that the ring is quite young, implies that our detection of it was an exceedingly unlikely event. The satellites Amalthea and Thebe, embedded near the ring's outer edge, are obvious candidates for source bodies; micrometeoroids impact their surfaces, injecting dust into the ring system<sup>1</sup>. Due to its larger escape velocity, Amalthea is only  $\sim 1/10$  as effective in this role as Adrastea, which contributes to the bright ring<sup>1,4</sup>. However, Amalthea and Thebe's ejecta should evolve outwards under plasma drag, and so cannot fully explain the gossamer ring.

Unseen bodies provide a plausible alternative source, and these must extend across the synchronous orbit for the ring to also appear on both sides. Since sputtering and plasma drag act

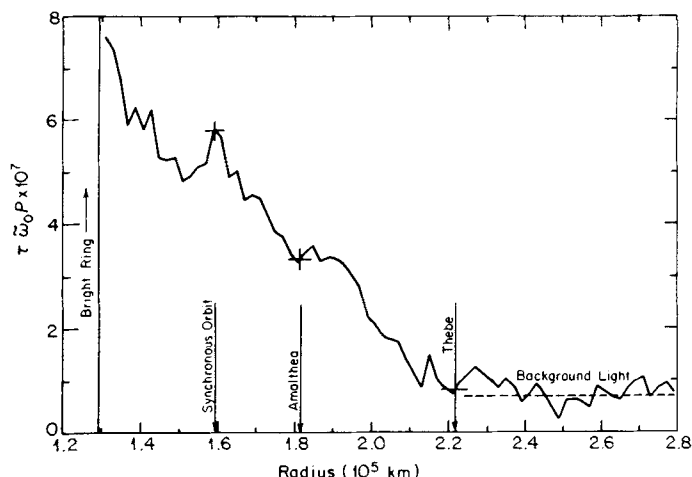


**Fig. 3** A radial profile of the external jovian ring. The vertical axis is in non-dimensional units of  $\tau \tilde{\omega}_0 P$ , where  $\tau$  is normal optical depth,  $\tilde{\omega}_0$  is single-scattering albedo and  $P$  is the phase function at scattering angle  $\theta$ . This quantity is directly proportional to measured intensity, but eliminates various projection effects<sup>4</sup>.

on comparable timescales, we expect a steady decrease in brightness with distance from any source region. This may account for the ring's observed linear decay beyond synchronous orbit, implying that the source bodies are confined to a much narrower radial region than are the visible grains.

The bright feature at synchronous orbit appears surprising at first, since plasma drag drives material away from this location, not towards it. However, here the ring material and plasma corotate, so the plasma drag force vanishes. Hence, material injected into the ring at this orbit will evolve away more slowly (probably inward under the weak Poynting-Robertson drag force<sup>1</sup>) than that introduced elsewhere. If the source body population straddles synchronous orbit, then this brightness enhancement is to be expected.

Another mysterious aspect of this ring is its limited vertical extent,  $<4,000$  km. The halo is thickened by perturbations from Jupiter's inclined magnetic field, acting on its tiny, charged grains<sup>1,2,8</sup>; the same processes should also be acting in this ring. The one important difference is the strength of the magnetic forcing. The dipole field component in the exterior ring is smaller by a factor of  $\sim 3$ , while higher-order moments are reduced even further. At the same time, grain velocities with respect to the

corotating field are smaller here, close to synchronous orbit. It is consistent with this trend that strong Lorentz resonances seem to have a major role in the halo<sup>8</sup>, but are not present in the gossamer ring. These circumstances combine to reduce the magnetic perturbations, and hence the ring's vertical extent, by a factor of at least 10 compared with the halo. This places the ring's thickness within its measured upper limit.

Although this gossamer ring remains enigmatic, it may at least have a dynamical counterpart at Saturn. A very faint outward extension to Saturn's A ring has been discovered by statistical analysis of the Voyager 2 photopolarimeter stellar occultation data<sup>9</sup>. Like its jovian analogue, it extends from a much brighter ring (Ring A) outwards to the vicinity of a satellite (Atlas), while decreasing continuously in optical depth. Its mean  $\tau$  is  $\sim 2\%$  of the outer A ring value. However, in its radial width ( $\sim 900$  km) and overall optical depth ( $\sim 0.01$ ), this ring is very different from the faint outer ring at Jupiter. Additional material at much lower optical depths, identified using image processing techniques similar to those described herein, fills the entire region between the A and F rings<sup>10</sup>. Whether these structures truly have a common dynamical basis is unknown, but surely searches should be made for similar material at Uranus.

We thank G. Garneau, C. Hansen, and especially S. A. Collins for help with the data processing, and W. Fillius for helpful discussions. M.R.S. and J.A.B. were supported in part by NASA grant NAGW-310.

Received 8 May; accepted 18 June 1985.

1. Burns, J. A., Showalter, M. R. & Morfill, G. E. in *Planetary Rings* (eds Greenberg, R. & Brahic, A.) 200-272 (University of Arizona Press, Tucson, 1984).
2. Jewitt, D. C. & Danielson, G. E. *J. geophys. Res.* **86**, 8691-8697 (1981).
3. Owen, T. *et al. Nature* **281**, 442-446 (1979).
4. Showalter, M. R. thesis Cornell Univ. (1985).
5. Humes, D. H., Alvarez, J. M., O'Neal, R. L. & Kinard, W. H. *J. geophys. Res.* **79**, 3677-3684 (1974).
6. Acuña, M. H. & Ness, N. F. *J. geophys. Res.* **81**, 2917-2922 (1976).
7. Elliott, J. & Kerr, R. *Rings: Discoveries from Galileo to Voyager*, 93-95 (MIT Press, Cambridge, 1985).
8. Burns, J. A., Schaffer, L. E., Greenberg, R. J. & Showalter, M. R. *Nature* **316**, 115-119 (1985).
9. Graps, A. L., Lane, A. L., Horn, L. J. & Simmons, K. E. *Icarus* **60**, 409-415 (1984).
10. Burns, J. A., Cuzzi, J. N. & Showalter, M. R. *Bull. Am. astr. Soc.* **15**, 1013-1014 (1983).

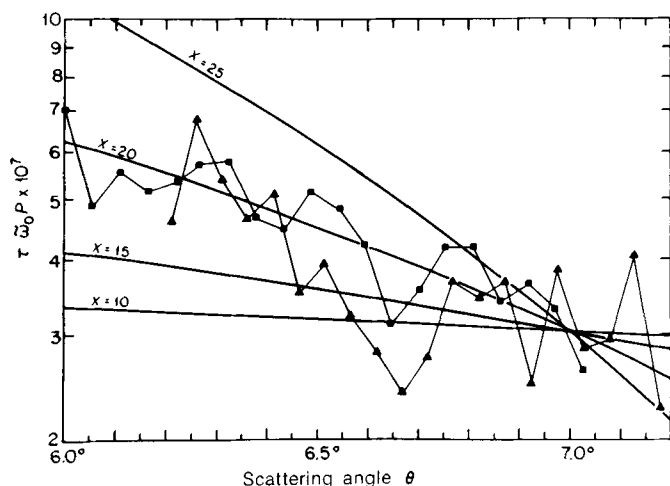


**Fig. 4** Variations in ring intensity with scattering angle  $\theta$ , measured at constant radius. Despite the point scatter, a brightening trend is revealed; a straight-line fit to the data yields a slope of  $0.7 \pm 0.1 \text{ mag deg}^{-1}$ . Phase functions for particles of size parameter  $X$  are shown for comparison<sup>4</sup>, where  $X$  is defined as the ratio of particle circumference to wavelength ( $0.5 \mu\text{m}$ ).  $\blacktriangle$ , Near arm;  $\blacksquare$ , far arm.

## High time-resolution observations of periodic frictional heating associated with a Pc5 micropulsation

G. Crowley, N. Wade, J. A. Waldock, T. R. Robinson & T. B. Jones

Department of Physics, Leicester University, University Road, Leicester LE1 7RH, UK

Geomagnetic micropulsations are fluctuations of the Earth's magnetic field on time-scales ranging from a few seconds to several minutes and with amplitudes varying between a few and several hundred nanotesla. In the inner magnetosphere, where the Earth's magnetic field lines are closed, the oscillations can adopt a standing wave pattern with a scale size comparable to the dimensions of the magnetospheric cavity. These hydromagnetic waves constitute one of the primary mechanisms for the transfer of energy from the outer regions of the magnetosphere to the high-latitude ionosphere during geomagnetic substorms. In the ionosphere, Joule heating is thought to be the dominant damping process for the pulsations and the rate of energy dissipation during a typical event<sup>1</sup> is of the order of  $10^9$  W. By means of the EISCAT (European Incoherent Scatter) radar facility it has been possible to measure directly the ionospheric ion-temperature and ion-velocity fluctuations during a micropulsation. The relationship predicted by the theory of Joule heating for these two parameters is confirmed in detail by the high time-resolution results reported here.